MANAS Journal of Engineering
ISSN 1694-7398 | e-ISSN 1694-7398

Volume 10, Issue 2, (2022) Pages 159-164
https://doi.org/10.51354/mjen. 1164604

Design and analysis of switched reluctance motor with FEM based Ansys-Maxwell

Yıldırım Özüpak

Dicle University, Silvan Vocational School, Electrical Department, Diyarbakır, yildirimozupak@gmail.com, ORCID:0000-0001-8461-8702

ABSTRACT

In this study, radial forces that create noise, which is a fundamental problem in Switched Reluctance Motor (SRM), are investigated. Since radial force causes stator vibrations and noise caused by magnetic field, a new switched reluctance motor model with increased stator and rotor poles has been designed in order to reduce the radial force acting on the rotor poles. In addition, a structure with high torque and low leakage flux compared to conventional winding structure has been proposed for Switched Reluctance Motors (SRM). The windings of the designed SRM are placed in layers, insulated from each other. Rotor poles are formed to move on both sides of each phase winding. Thus, the flux that will occur in the phase windings axially completes its circuit from the stator poles and the rotor poles. This designed ARM model has been examined by Finite Element Method (FEM. The proposed motor geometry has been analyzed with ANSYS Maxwell-3D, which performs FEM-based solution), and parametric analysis with ANSYS-RMxprt.

ARTICLE INFO

Research article

Received: 19.08.2022
Accepted: 8.12.2022

Keywords:
SRM,
Maxwell-3D,
FEM

1. Introduction

Simple and robust construction, high efficiency and low cost are the generally accepted advantages of inverter circuit switched reluctance motors. Despite being extensively studied by researchers, the widespread use of switched reluctance motors in industry and household appliances has not yet been possible.

Switched reluctance motor has two drawbacks: torque ripple and acoustic noise. While the switched reluctance motor is running, vibrations occur in the stator as a result of radial forces and acoustic noise occurs. Compared to electronically controlled drives such as induction motors and permanent magnet synchronous motors, the acoustic noise level in ARM is higher.

The vibrations in the stator are caused by the torque generation mechanism of the switched reluctance motor. When current flows through a phase winding, a torque is produced that pulls the rotor to its smallest reluctance position. In order not to produce negative torque, the current is drawn to zero in a position close to the coincident position. The force acting on the rotor pole consists of two components, the tangential force component and the normal force component. The tangential force component produces torque in the rotor. The normal force component creates vibration in the stator. In the coincidence position, no moment is produced, so the tangential force component is zero. However, in the coincident position, the normal force component reaches its maximum value. When the normal force pulling the rotor poles is small over the bearings on which the rotor shaft is placed, the change in inductance is larger, and thus large moments are produced. As the number of stator and rotor poles increases, the difference between the lowest phase inductance value and the largest phase inductance value becomes smaller, and therefore the torque produced for the same phase current becomes smaller.

Industrial interest in switched reluctance motors (ARM) dates back to the 1800s [1]. The switched reluctance machine was first used by Dawidson in Scotland in 1838 to move a locomotive [2, 3]. In the 1920s, a stepper motor was invented by C.L.Walker, which has the features of today's ARMs. In 1969 S.A. Nasar revealed the first basic features of the classical ARM [4]. Bedford and Hoft simultaneously switched stator winding currents to the rotor position, shaping today's modern ARMs and pioneering the effective use of semiconductor elements in ARM technology [5, 6]. They also conducted research on rotor and stator pole geometries and power electronics converter structures.

Miller brought the computer aided design approach to ARM design in 1991 and worked on optimum design

parameters [7]. A 6/4 pole ratio ARM operating with high voltage was designed by Miles [8]. Materu and Krishnan tried to find the losses of the 6/4 pole configuration prototype ARM produced, and tried to produce general expressions by obtaining the stator current and voltage waveforms. It is used for 100 HP ARM hybrid vehicles produced by Khwaja M.Rahman. It has been observed that the acceleration time of the designed ARM is much better than the asynchronous motor of the same power [9].

In recent years, significant developments have been made in switched reluctance motor designs, especially the design optimization results obtained in the stator structure have gained qualifications to lead to interesting designs. Significant developments in ARM design have caused these motors to take their place in robotic applications.
In this study, SRM was designed and analyzed on the ANSYS-RMxprt-Maxwell integrated platform. Maxwell-2D was used for RMxprt magnetic field analysis for parametric analyses. The results obtained were compared with the studies on this subject in the literature. The results were found to be satisfactory.

2. Material and method

2.1. Design SRM structure

One of the many studies on the optimum design of SRM was done by Miller. It is necessary to make the most appropriate choice by considering many criteria in switched reluctance motor designs made to reduce noise and prevent fluctuation in torque. One of the changes made on the geometric structure of the SRM in order to reduce the radial force was to increase the number of stator and rotor poles. When the number of stator and poles is increased, the radial force acting on the rotor poles decreases for the same peak torque, so the noise generated as a result of vibrations in the SRM decreases. However, as the number of stator and rotor poles increases, the iron losses due to the increasing switching frequency of the phases increase somewhat. On the other hand, as the number of rotor and stator poles increases, the flux paths of the phases will shorten, and there will be a decrease in iron losses due to the path followed by the flux.

2.2. SRM Electrical equivalent circuit

In the designed SRM, the flux does not pass from the stator pole end to the air gap and then to the rotor pole, as in other conventional SRMs. Here, the flux passes from the winding to the stator pole and from there to the side surface of the rotor pole by air. Therefore, the flux path through which the flux can pass has been widened. Thus, the attraction force between the stator and rotor is increased. The working principle of SRMs is based on the reluctance force, and it is realized in the form of pulling the flux in the magnetic circuit of the free-moving, protruding rotor by applying force to the smallest reluctance position where it can find the easiest way. Figure 1 shows the equivalent circuit for a single phase of the SRM.

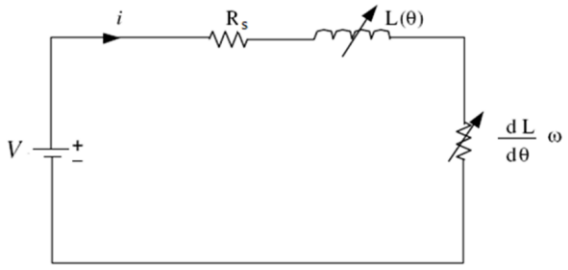

Figure 1. *Equivalent circuit diagram of one phase of SRM*

In the circuit given in Figure 1, Rs represents the stator winding resistance and L inductance value for each phase. Here, the voltage value applied to each phase can be given as in equation (1).

$$v = R_s i + \frac{d\lambda(\theta,i)}{dt} \quad (1)$$

$$\lambda = L(\theta,i)i \quad (2)$$

It can be expressed as. The input power can be expressed as given in equation 3.

$$P_i = vi = R_s i^2 + i^2 \frac{dL(\theta,i)}{dt} + L(\theta,i) i \frac{di}{dt} \quad (3)$$

$$\frac{d}{dt}\left(\frac{1}{2}L(\theta,i)i^2\right) = L(\theta,i)i\frac{di}{dt} + \frac{1}{2}i^2\frac{dl(\theta,i)}{dt} \quad (4)$$

Equations can be written. Starting from these equations, the input power can be written as in equation (5).

$$P_i = R_s i^2 + \frac{d}{dt}\left(\frac{1}{2}L(\theta,i)i^2\right) + \frac{1}{2}i^2\frac{dl(\theta,i)}{dt} \quad (5)$$

As can be clearly seen from Equation (5), the input power consists of the sum of the winding loss power given by the expression $R_s i^2$, the rate of change of the field energy given by the expression p($\frac{1}{2}L(\theta,i)i^2$), and the air gap power given by the $\frac{1}{2}i^2$ p$L(\theta,i)$expression. If the rotor position and speed terms are substituted in the time expression for the air gap power;

$$T_e = \frac{\theta}{w_m} \quad (6)$$

$$P_{ag} = \frac{1}{2}i^2\frac{dl(\theta,i)}{dt} = \frac{1}{2}i^2\frac{dL(\theta,i)}{d\theta}\frac{d\theta}{dt} \quad (7)$$

$$P_{ag} = \frac{1}{2}i^2\frac{dL(\theta,i)}{d\theta}w_m \quad (8)$$

expression is obtained.

Air gap power depends on electromagnetic torque and speed,

$$P_{ag} = T_e w_m \quad (9)$$

$$T_e = \frac{1}{2} i^2 \frac{dL(\theta,i)}{d\theta} \quad (10)$$

It is obtained as [7]

3. Result and discussion

3.1. SRM's magnetic analysis and results

Magnetic analyzes of SRM were carried out in two dimensions in Ansys Maxwell program. Transient analyzes were performed on the designed model. While creating the model, Dirichlet boundary condition is assigned to the outermost edge surfaces of a region, to the stator outer diameter and stator package length. In Figure 2, the designed model divided into networks is shown.

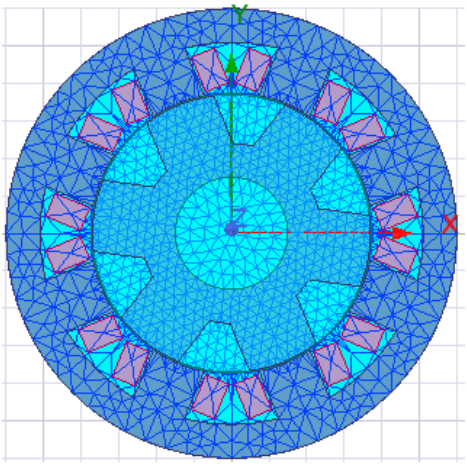

Figure 2. *Mesh structure of the designed motor*

SRM motors are motors that can be switched by position control. That is, after the first position information of the motor is received, a voltage is applied to the windings. The switching circuit drawn in the simplorer program in Figure 3 is used for transient analysis in magnetic simulation. This circuit performs a realistic analysis using the magnetic circuit model.

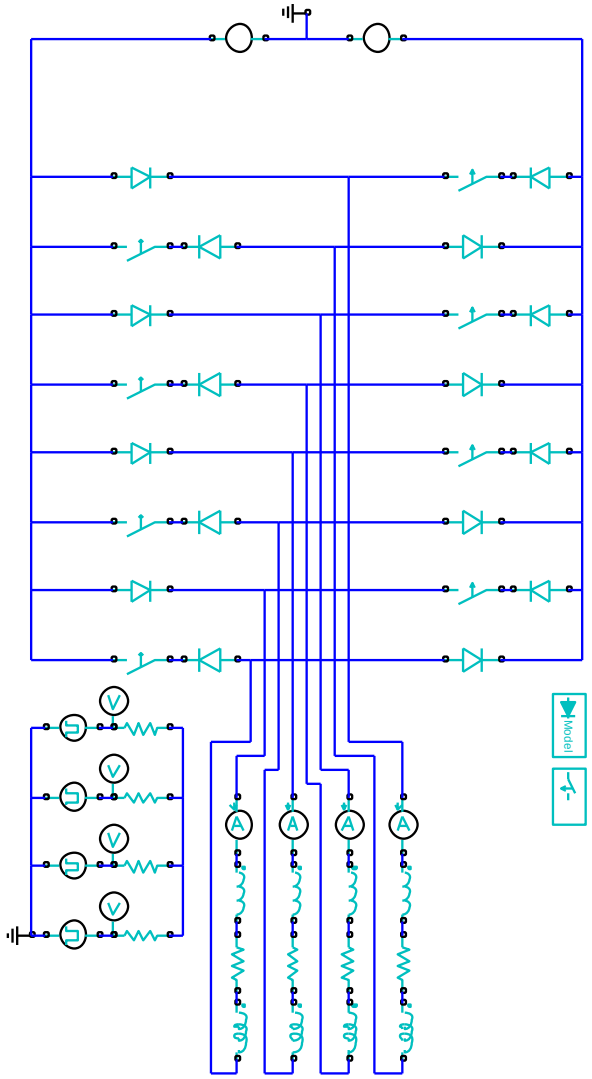

Figure 3. *Driver circuit used for magnetic field analysis of SRM*

Steel 1010 B-H curve of magnetic material used for rotor and stator in the model is given in Figure 9. In analytical calculations, the relative magnetic permeability (μ_r) of the magnetic material is taken as constant.

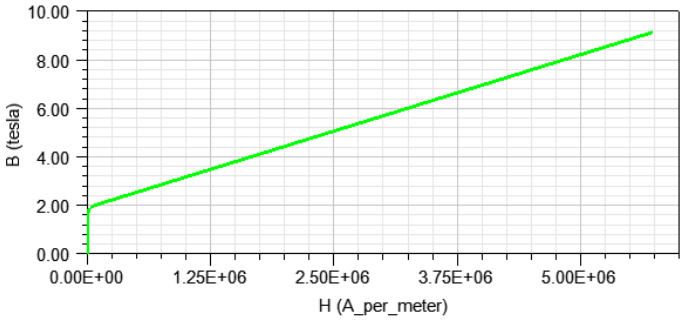

Figure 4. *Steel 1010 B-H curve used as stator and rotor material*

As a result of the magnetic analysis of the designed SRM, magnetic analysis results at different locations were obtained. The vectorial representation of the magnetic flux value in the case of the maximum gap between the stator and rotor poles is given in Figure 5.

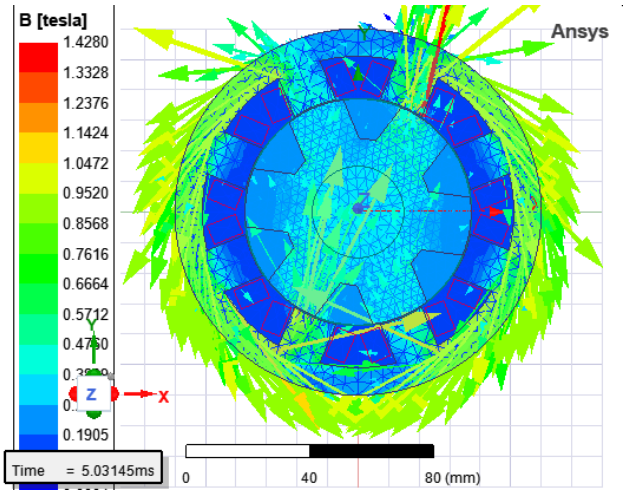

Figure 5. *Vectorial distribution of magnetic flux values between stator and rotor poles*

The windings of the SRM are triggered individually or together at certain angles to reduce torque fluctuations thanks to the designed encoder. In Figure 6, the magnetic flux in the rotor, stator and air gap is shown as vector when the windings are energized. If Figure 6 is examined, it can be seen that the leakage fluxes in the air gap are negligible.

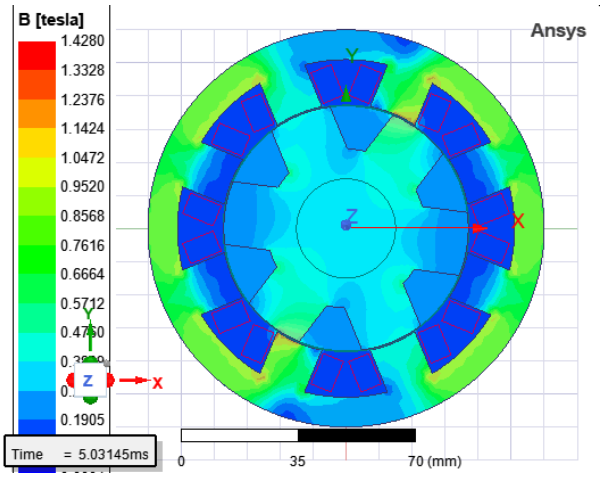

Figure 6. *Magnetic flux distribution on model*

As a result of the analysis of SRM, torque, inductance, flux, current and voltage curves were obtained. If the poles are too far from each other, the inductance is at the lowest value, and when the poles are in the same position, the inductance reaches its maximum value. The windings are energized by looking at the minimum and maximum values in this curve.

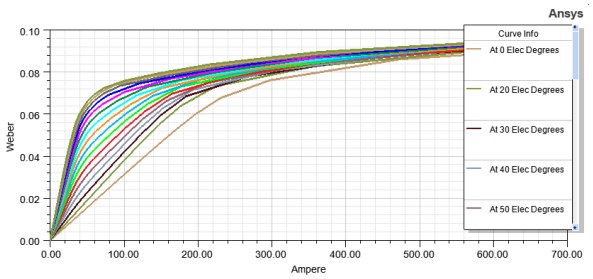

Figure 7. *Flux-airgap of the SRM*

The EMF values induced on the windings as a result of the parametric magnetic analysis are shown in Figure 8. The supply of the motor windings is provided by triggering the switches according to the angular velocity position information obtained in the driver circuit drawn in the Simplorer program. If the induced voltage curves are examined, the negative voltages are given back to the source together with the induced back emfs in the windings. Figure 9 shows the flux values of the windings as a result of the voltage applied to the windings of the SRM. The currents drawn by the motor windings are shown in Figure 10 as a current-time graph.

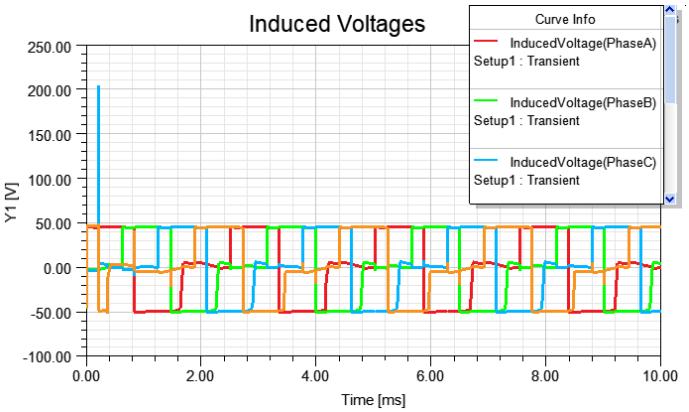

Figure 8. *Graph of voltage induced in windings*

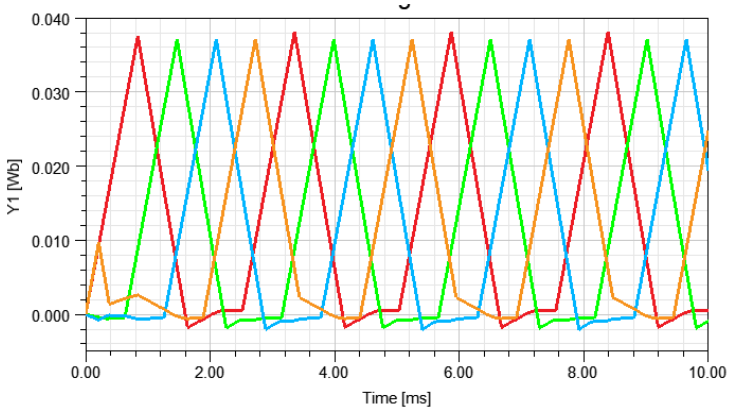

Figure 9. *Flux values in the windings of the SRM*

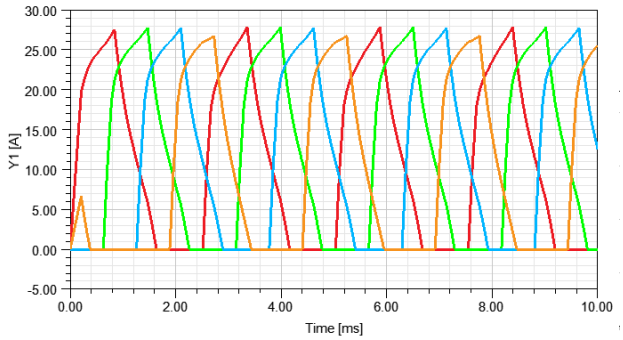

Figure 10. *SRM windings current vurves*

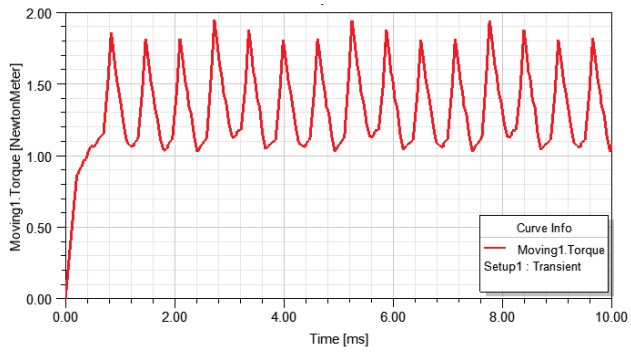

Figure 11. *SRM speed-time curve*

By energizing the SRM windings in this way, the motor speed reaches 429.77 rpm in a very short time and remains constant there. Velocity-time graph is given in Figure 11. While designing the SRM, parametric analyzes were carried out on motor dimensions, and parametric analyzes were made in the form of optimization of rotor and stator pole dimensions. Rotor and stator pole combinations that can give the most suitable torque value were tried and parametric analyzes were carried out. While performing the analysis, variables such as voltage, speed, and load were kept constant, and a parametric analysis was carried out by changing only the rotor and stator geometry. As can be seen in the figure, the torque value produced by the motor increased to the maximum at the peak values, but did not decrease to the minimum value too much. In other words, torque fluctuation is less compared to other structures.

4. Conclusion

Recently, many researches and studies are carried out on the design and application of switched reluctance motors. When the studies are examined, it can be concluded that these academic studies are on the structural design of the engine and the design of the control circuit. In this study, SRM was designed and analyzed. The designed SRM structure was modeled with the ANSYS-Maxwell 2D program. Rotor time transient analyzes were made and torque, phase inductance and magnetic flux density values were obtained. The torque SRM length is maximized in the design. It has been observed that the torque graph obtained is in SRM torque characteristic and torque fluctuation occurs. It is recommended to switch phases together in certain positions to avoid torque fluctuations. It is possible to further reduce the ripples by increasing the number of phases of the motor. Controlling the prototype obtained by optimizing the design with a more skilled driver will be useful in demonstrating the capabilities of the SRM design.

References

[1]. Irwin, J. D., 2001. “Switched Reluctance Motor Drives; Modeling, Simulation, Analysis, Design, and Applications”, Series Editor, Auburn University, Alabama, A.B.D.

[2]. Vijayraghavan, P., 2001. “Design of Switched Reluctance Motors and Development of a Universal Controller for Switched Reluctance and Permanent Magnet Brushless DC Motor Drives”, Faculty of the Virginia Polytechnic Institute and State University, Blacksburg, Virginia,

[3]. Miller, T.J.E., 1993. “Switched Reluctance Motors and their Control”, Magna Physics Publishing and Clarendon Press, Oxford, İngiltere,

[4]. Nasar, S.A., 1969. “DC Switched Reluctance Motor”, Proc. IEE, Cilt 116, No 6, 1048–1049,

[5]. Lawrenson, P.J., 1980.Stephenson, J.M., Blenkinsop, P.T., Corda, J. and Fulton, N.N., “Variable-speed Switched Reluctance Motors”, Proc. IEE, Cilt 127, No 4, 253–265,

[6]. Byrne, J. and Lacy, J.C.; 1976. “Electrodynamic system comprising a variable reluctance machine”, U.S. Patent 3956678.

[7]. Miller T. J. E., 2001. “Electronic Control of Switched Reluctance Machines”, Oxford, İngiltere, 48-56,

[8]. Miles A.R. 1991. “Design of a 5 MW, 9000V Switched Reluctance Motor”, IEEE Trans. Energy Conversion, Cilt 6, 484–491,

[9]. Khwaja M. R., 2000. “Advantages of Switched Reluctance Motor Applications to EV and HEV: Design and Control Issues”, IEEE Transactions on Industrial Applications, Cilt 36, No 1, 1-4,

[10]. S. S. Ahmad, E. Dhar, P. Kumar, and G. Narayanan, 2016. “Electromagnetic design of a 5-kW, 10,000 rpm switched reluctance machine,” in 2016 7th India

International Conference on Power Electronics (IICPE), 1–6.

[11]. S. Allirani, H. Vidhya, T. Aishwarya, T. Kiruthika, and V. Kowsalya, 2018. “Design and Performance Analysis of Switched Reluctance Motor Using ANSYS Maxwell,” in 2018 2nd International Conference on Trends in Electronics and Informatics (ICOEI), pp. 1427–1432.

[12]. Uzhegov, N.; Barta, J.; Kurfurst, J.; Ondrusek, C.; Pyrhonen, J. 2017. Comparison of High-Speed Electrical Motors for a Turbo Cir-culator Application. IEEE Trans. Ind. Appl., 53, 4308–4317.

[13]. Lim, M.-S.; Kim, J.-M.; Hwang, Y.S.; Hong, J.-P. 2017. Design of an ultra-high-speed permanent-magnet motor for an electric turbocharger considering speed response characteristics. IEEE/ASME Trans. Mechatron., 22, 774–784.

[14]. Kocan, S.; Rafajdus, P. 2019. Dynamic model of high speed switched reluctance motor for automotive applications. Transp. Res. Procedia, 40, 302–309..